



# UNIVERSITÀ DI PARMA

## ARCHIVIO DELLA RICERCA

University of Parma Research Repository

Virtual Screening and Biological Validation of Novel Influenza Virus PA Endonuclease Inhibitors

This is the peer reviewed version of the following article:

*Original*

Virtual Screening and Biological Validation of Novel Influenza Virus PA Endonuclease Inhibitors / Pala, Nicolino; Stevaert, Annelies; Dallochio, Roberto; Dessi, Alessandro; Rogolino, Dominga; Carcelli, Mauro; Sanna, Vanna; Sechi, Mario; Naesens, Lieve. - In: ACS MEDICINAL CHEMISTRY LETTERS. - ISSN 1948-5875. - 6:(2015), pp. 866-871. [10.1021/acsmedchemlett.5b00109]

*Availability:*

This version is available at: 11381/2795696 since: 2021-10-04T09:10:54Z

*Publisher:*

American Chemical Society

*Published*

DOI:10.1021/acsmedchemlett.5b00109

*Terms of use:*

Anyone can freely access the full text of works made available as "Open Access". Works made available

*Publisher copyright*

note finali coverpage

(Article begins on next page)

# Virtual Screening and Biological Validation of Novel Influenza Virus PA Endonuclease Inhibitors

Nicolino Pala,<sup>\*,†</sup> Annelies Stevaert,<sup>‡</sup> Roberto Dallochio,<sup>§</sup> Alessandro Dessì,<sup>§</sup> Dominga Rogolino,<sup>||</sup> Mauro Carcelli,<sup>||</sup> Vanna Sanna,<sup>†</sup> Mario Sechi,<sup>†</sup> and Lieve Naesens<sup>\*,‡</sup>

<sup>†</sup>Dipartimento di Chimica e Farmacia, Università di Sassari, Via Vienna 2, 07100 Sassari, Italy

<sup>‡</sup>Rega Institute for Medical Research, KU Leuven, Minderbroedersstraat 10, B-3000 Leuven, Belgium

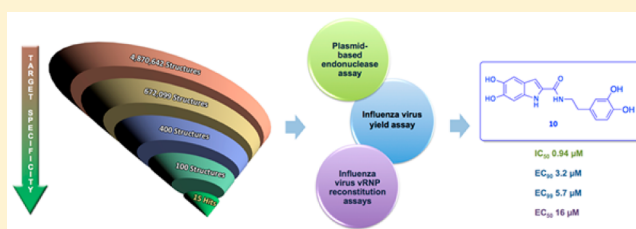
<sup>§</sup>Istituto di Chimica Biomolecolare, CNR–Consiglio Nazionale delle Ricerche, Sassari, 07100 Li Punti Italy

<sup>||</sup>Dipartimento di Chimica, Università di Parma, Parco Area delle Scienze 17/A, 43124 Parma, Italy

## Supporting Information

**ABSTRACT:** The influenza virus RNA-dependent RNA polymerase complex (RdRp), a heterotrimeric protein complex responsible for viral RNA transcription and replication, represents a primary target for antiviral drug development. One particularly attractive approach is interference with the endonucleolytic “cap-snatching” reaction by the RdRp subunit PA, more precisely by inhibiting its metal-dependent catalytic activity which resides in the N-terminal part of PA (PA-Nter). Almost all PA inhibitors (PAIs) thus far discovered bear pharmacophoric fragments with chelating motifs able to bind the bivalent metal ions in the catalytic core of PA-Nter. More recently, the availability of crystallographic structures of PA-Nter has enabled rational design of original PAIs with improved binding properties and antiviral potency. We here present a coupled pharmacophore/docking virtual screening approach that allowed us to identify PAIs with interesting inhibitory activity in a PA-Nter enzymatic assay. Moreover, antiviral activity in the low micromolar range was observed in cell-based influenza virus assays.

**KEYWORDS:** Influenza virus PA endonuclease, polymerase, metal chelation, pharmacophore–structure virtual screening, PA inhibitors (PAIs), dihydroxy-1H-indole-2-carboxamides



Seasonal influenza A and B virus infections are a worldwide concern, causing each year 3–5 million severe infections and 250000–500000 fatalities.<sup>1</sup> The current influenza vaccines are only partially effective in some populations<sup>2</sup> and require annual updating. Also, antiviral therapy is not fully satisfactory because only two classes of antiviral drugs are available. Resistance is already widespread for the M2 blockers and increasingly recognized for the neuraminidase inhibitors.<sup>3,4</sup> Hence, there is an urgent need for new anti-influenza drugs.

The influenza virus genome consists of eight negative-sense RNA segments which encode at least 17 viral proteins. Transcription and replication of viral RNA (vRNA) is carried out by the viral RNA-dependent RNA polymerase (RdRp).<sup>5</sup> The crystal structure of the large (~250 kDa) RdRp complex was reported very recently.<sup>6,7</sup> It is composed of three subunits, PB1, PB2, and PA, which are highly conserved among influenza A and B viruses. During vRNA transcription, the RdRp cleaves host pre-mRNAs at a distance of 10–15 nucleotides from their 5'-capped terminus.<sup>8</sup> While cap binding is performed by PB2, the endonuclease activity resides in the N-terminal domain of PA (PA-Nter; containing residues 1 to ~195).<sup>9,10</sup> After endonuclease cleavage, the short 5'-capped RNA serves as primer for viral mRNA synthesis by the PB1 unit and,

subsequently, the viral mRNAs are translated by the host cell machinery.

Inhibition of the PA endonuclease appears a powerful strategy to suppress influenza virus replication.<sup>9–12</sup> In the last two decades, several small molecule PA inhibitors (PAIs) have been discovered.<sup>13–21,24–26</sup> Structurally diverse classes of potential PAIs have been identified (Figure 1) such as flutimide and derivatives,<sup>15,17</sup> N-hydroxamic acids and N-hydroxyimides,<sup>16</sup> and epigallocatechin gallate (EGCG).<sup>21</sup> Neither of these have comparable antiviral potency as L-742,001<sup>14</sup> and closely related DKAs. More recently, a series of hydroxypyridazinones and hydroxypyridinones<sup>18,20</sup> were identified with particularly strong activity toward the PA-Nter enzyme.

The catalytic core of PA-Nter contains a (P)DX<sub>N</sub>(D/E)XK motif formed by D108, E119, a proline (influenza A) or alanine (influenza B) at position 107, and K134 or K137.<sup>9,10</sup> It comprises a histidine (H41) and a cluster of three acidic residues (E80, D108, E119), conserved in all influenza viruses, which coordinate (together with I120) one,<sup>10</sup> two,<sup>9</sup> or three<sup>18</sup> divalent metal ions (Mg<sup>2+</sup> or Mn<sup>2+</sup>, with Mg<sup>2+</sup> being the

Received: March 14, 2015

Accepted: June 18, 2015

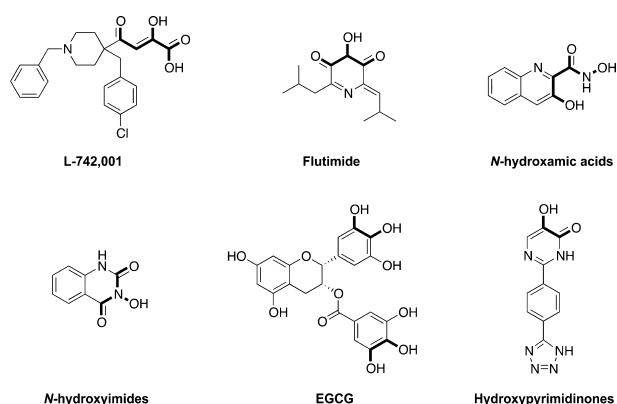


**Figure 1.** Representative influenza virus endonuclease inhibitors. The putative metal-chelating chemotype is marked in bold.

69 probable cofactor *in vivo*<sup>22</sup>). To date, 35 crystal structures  
70 related to the influenza virus PA endonuclease have been  
71 deposited in the RCSB Protein Data Bank,<sup>23</sup> and more than 20  
72 are in complex with an inhibitor. In combination with  
73 biochemical studies, these structural studies support the  
74 assumption that all PAIs thus far identified inhibit the PA  
75 enzyme through chelation of its metal cofactor(s) within the  
76 catalytic core. The availability of these complementary PA-Nter  
77 crystal structures has created the opportunity to rationally  
78 design PAIs with novel chelating structures and enhanced  
79 enzyme binding properties to improve antiviral activity in cell  
80 culture.<sup>18,20,24–26</sup>

81 Indeed, together with other traditional strategies, virtual  
82 screening (VS) is recognized as a powerful tool in drug  
83 discovery,<sup>27,28</sup> as previously explored by us to identify some  
84 novel and potent metalloenzyme inhibitors.<sup>29</sup> To be effective,  
85 the VS method should have a proper balance between  
86 predictability and time consumption. With regard to the PA  
87 enzyme, only a few examples of computer-aided inhibitor  
88 design have thus far been reported, in which molecular diversity  
89 was explored to recognize unique pharmacophores different  
90 from the DKA scaffold.<sup>30,31</sup> Herein, we present a coupled  
91 pharmacophore/docking virtual screening approach that  
92 allowed us to identify novel PAIs with interesting inhibitory  
93 activity in a PA-Nter enzymatic assay, as well as antiviral activity  
94 in cell-based influenza virus yield and vRNP reconstitution  
95 assays.

96 The outline of the experimental plan was as follows. First, a  
97 hybrid library of roughly 5 million compounds was built by  
98 merging the Clean Lead Database retrieved from ZINC and an  
99 in-house database of compounds bearing metal chelating  
100 functionalities, hence having the potential to inhibit PA-Nter  
101 on the basis of their previously evaluated activities against other  
102 metalloenzymes such as HIV-1 integrase and carbonic  
103 anhydrases.

104 Second, a suitable pharmacophore model was obtained.  
105 Generation of consistent models depends on the quality of  
106 both training and testing sets mainly in terms of structural  
107 diversity. As already shown by Parkes<sup>32</sup> and Kim,<sup>33</sup> the minimal  
108 pharmacophore motif is composed of two or three donor (i.e.,  
109 oxygen or nitrogen) atoms capable of chelating the two metal  
110 ions. Besides, the spatial disposition of these metal ligator (ML)  
111 moieties is critical to achieve effective inhibition of the influenza  
112 virus PA endonuclease. In particular, the oxygens should be  
113 displaced at the vertices of a triangle with dimensions of 2.60–  
114 2.80, 2.60–2.80, and 4.50–5.50 Å for the model proposed by

Parkes,<sup>32</sup> and of 2.56–2.87, 2.22–2.62, and 3.49–4.51 Å for  
115 that put forward by Kim.<sup>33</sup> Our best three pharmacophore  
116 models shown in Figure 2 (PH4-2, PH4-3, and PH4-9) were in  
117

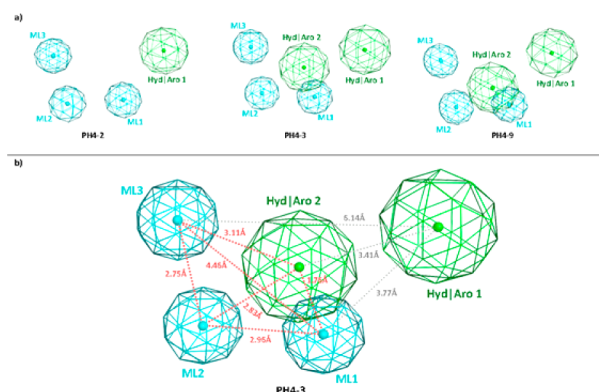


**Figure 2.** Influenza virus PA endonuclease pharmacophore models generated by MOE: (a) three-dimensional arrangement of the best three models; (b) representation of pharmacophore model PH4-3 that was selected for further study. Distances between centroids of the pharmacophore features are indicated as red or gray dashed lines.

118 nice agreement with these requirements (i.e., ML1-ML2-ML3  
119 interfeature distances are 2.75, 2.96, and 4.46 Å). Moreover,  
120 together with these three coordinating functionalities, our  
121 pharmacophore models combine one or two aromatic or  
122 hydrophobic regions that allow for additional stabilizing  
123 interactions of PAIs within the catalytic site (see Figure 2).  
124 Among these three models, model PH4-3 was found to  
125 properly distinguish between inactive and active compounds  
126 when applied to a test set of 50 structures (of which 10 were  
127 known to be active PAIs).

128 In the third step, a VS procedure on the above-mentioned  
129 database by means of combined pharmacophore-filtration and  
130 structure-based docking procedures was carried out. To speed  
131 up the process, the database was partitioned into 36 sublibraries  
132 that were processed in a parallel way using the software  
133 platform MOE.<sup>34</sup> Each library was first filtered using the  
134 Pharmacophore Search implemented in MOE. The derived  
135 five-points pharmacophore model PH4-3 was chosen as query,  
136 and all structures that matched at least four pharmacophore  
137 features were stored, thus realizing a ~7-fold reduction in the  
138 number of structures (see Figure 3). In the last steps of our  
139 *in silico* studies, the MOE Docking protocol was applied to the  
140 resulting libraries. After running the docking process, the best  
141 400 hits from all libraries were collected, and the top-ranked  
142 energy hits (about 100 molecules) with immediate availability  
143 were selected for the AutoDock refinement.

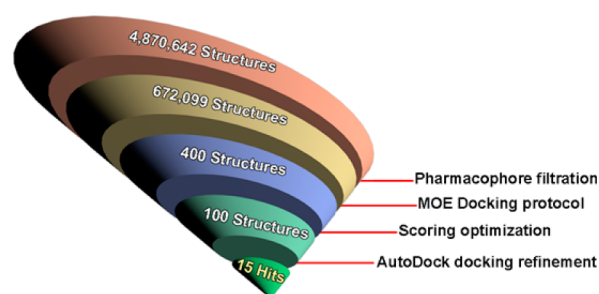
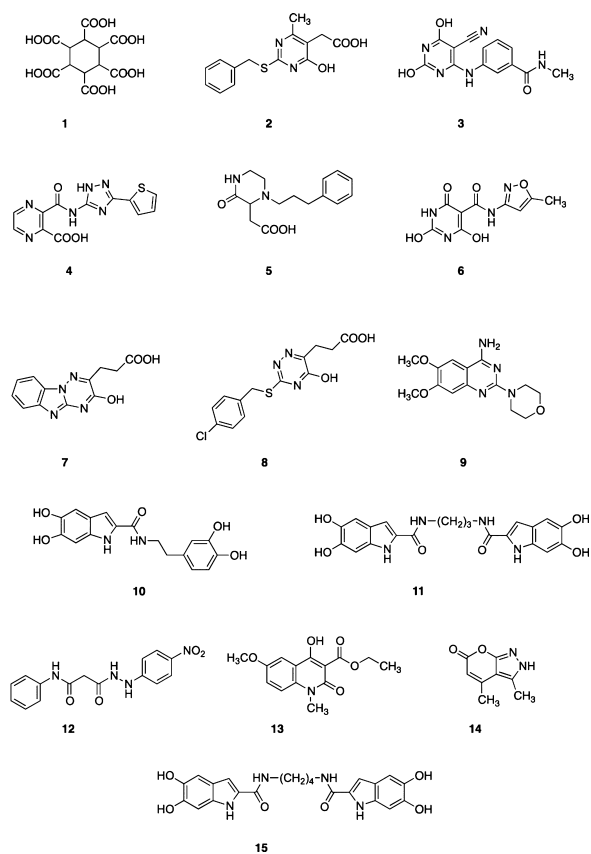


**Figure 3.** Scheme of the virtual screening approach.

144 Once these molecules were scored, clusterization by scaffold  
145 similarity was done, and compounds 1–15 (Chart 1) were

**Chart 1. Chemical Structures of the Hit Compounds Identified by the Virtual Screening Procedure**



146 finally selected for subsequent biological evaluation by three  
147 complementary methods, i.e., the enzymatic plasmid-based  
148 endonuclease assay with influenza virus PA-Nter and cell-based  
149 influenza vRNP reconstitution and virus yield assays.

150 To enable biological testing, compounds 1–8 were  
151 purchased while compounds 9–15 were retrieved from our  
152 collection.<sup>35–37</sup> Compounds 10, 11, and 15 have been

resynthesized in our laboratory using a previously described 153  
(and slightly modified) procedure,<sup>35</sup> which is depicted in 154  
Scheme 1. 10, 11, and 15 were obtained in moderate yields 155 s1  
(58%, 46%, and 65%, for 10, 11, and 15, respectively) by 156  
deprotection of the catechol moiety of the respective 157  
intermediates 21–23, with boron tribromide in dichloro- 158  
methane at low temperature (Scheme 1). Amides 21–23 were 159  
prepared by conversion of 2-carboxylic indole 16 to the acyl 160  
chloride 17, and next coupling with the appropriate amines. 161  
The key synthone 16 was easily obtained using a previously 162  
validated three-steps synthetic route.<sup>35</sup> 163

Among the 15 test compounds evaluated in the PA-Nter 164  
enzymatic assay (see Table 1), only compounds 10, 11, and 15 165 t1

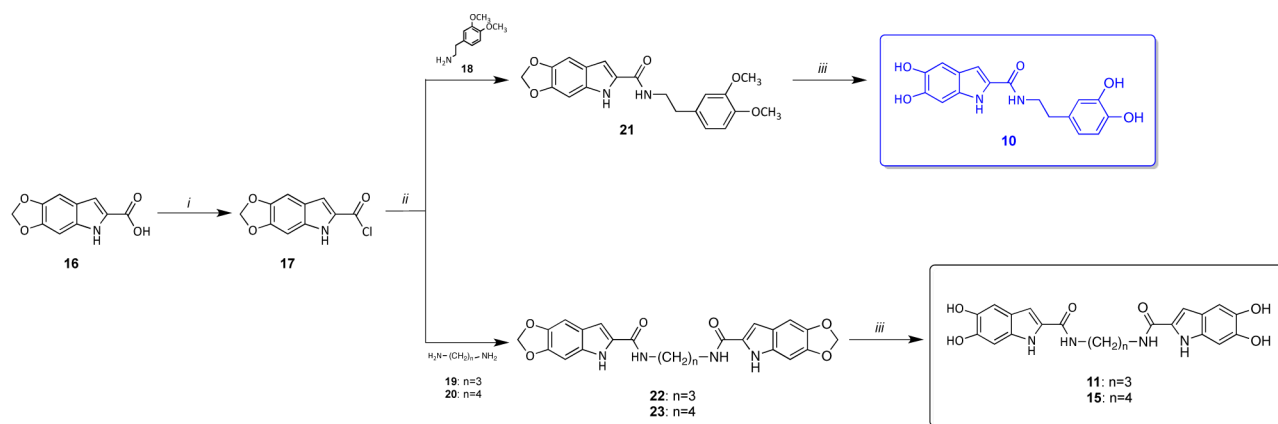
**Table 1. Activity of the 15 Test Compounds in the Plasmid-Based Enzymatic Assay with PA-Nter**

compd	IC <sub>50</sub> (μM) <sup>a</sup>	compd	IC <sub>50</sub> (μM) <sup>a</sup>
1	>500	9	>500
2	>500	10	0.94
3	>500	11	65
4	>500	12	>500
5	>500	13	>500
6	>500	14	>500
7	>500	15	7.0
8	>500	L-742,001	0.48

<sup>a</sup>IC<sub>50</sub>: 50% inhibitory concentration, calculated using nonlinear regression analysis. Values are the result of at least three independent experiments.

demonstrated inhibitory activity, with IC<sub>50</sub> values of 0.94, 65, 166  
and 7.0 μM for 10, 11, and 15, respectively. Interestingly, 10 167  
was only 2-fold less active than the prototype PAI L-742,001 168  
(IC<sub>50</sub>: 0.48 μM), which is one of the more active PAIs reported 169  
thus far. Compounds 10, 11, and 15 possess a similar 170  
dihydroxyindole scaffold structure which thus appears to be 171  
an important structural determinant for PA-Nter inhibitory 172  
activity. However, (pseudo) dimerization of this scaffold to 173  
obtain 11 and 15 leads to a significant reduction in activity. The 174  
dihydroxyindole scaffold of all three active compounds fits well 175  
within the pharmacophore model PH4-3 (see Supporting 176  
Information, Figure 1). 177

**Scheme 1. Synthesis of Compounds 10, 11, and 15<sup>a</sup>**



<sup>a</sup>Reagents and conditions: (i) PCl<sub>5</sub>, diethyl ether, rt, 2 h; (ii) diethyl ether, rt, 2 h; (iii) 1 M BBr<sub>3</sub> solution in CH<sub>2</sub>Cl<sub>2</sub>, –70 °C to –40 °C (for 10), or –70 °C to –0 °C (for 11 and 15), 4 h.

178 As far as antiviral activity in cell culture is concerned, all three  
179 compounds **10**, **11**, and **15** inhibited virus replication in a virus  
180 yield assay in influenza virus-infected MDCK cells, with  $EC_{90}$   
181 and  $EC_{99}$  values of 3.2 and 5.7  $\mu\text{M}$  for **10**, 32 and 73  $\mu\text{M}$  for **11**,  
182 and 6.3 and 12  $\mu\text{M}$  for **15** (see Table 2). It is remarkable that

**Table 2. Anti-Influenza Virus Activity of Selected Compounds 10, 11, and 15 in Cell-Based Influenza Virus Assays**

compd	virus yield assay in MDCK cells <sup>a</sup>			vRNP reconstitution assay in HEK293T cells <sup>a</sup>	
	$EC_{90}$ <sup>b</sup> ( $\mu\text{M}$ )	$EC_{99}$ <sup>b</sup> ( $\mu\text{M}$ )	$CC_{50}$ <sup>c</sup> ( $\mu\text{M}$ )	$EC_{50}$ <sup>d</sup> ( $\mu\text{M}$ )	$CC_{50}$ <sup>e</sup> ( $\mu\text{M}$ )
L-742,001	5.4 ± 0.3	8.4 ± 0.3	181	3.4	>100
<b>10</b>	3.2 ± 0.9	5.7 ± 1.6	≥50	16	110
<b>11</b>	32 ± 7	73 ± 6	>200	64	>200
<b>15</b>	6.3 ± 1.5	12 ± 3	>200	24	>200
ribavirin	6.8 ± 0.5	11 ± 1	>200	8.4	>200

<sup>a</sup>MDCK, Madin–Darby canine kidney cells; HEK293T cells, human embryonic kidney 293T cells. <sup>b</sup>Compound concentration ( $\mu\text{M}$ ) causing 1- $\log_{10}$  ( $EC_{90}$ ) or 2- $\log_{10}$  ( $EC_{99}$ ) reduction in virus yield at 24 h pi, as determined by real time RT-PCR. Values shown are the mean ± SEM of at least four experiments. <sup>c</sup> $CC_{50}$ , 50% cytotoxic concentration determined by MTS cell viability assay at 24 h. <sup>d</sup> $EC_{50}$ : 50% effective concentration, i.e. compound concentration producing 50% reduction in vRNP-driven firefly reporter signal, estimated at 24 h after transfection, and calculated by nonlinear regression analysis from data of 3 independent experiments.

183 derivatives **10** and **15** had a potency comparable to that of the  
184 reference compound L-742,001 (which had  $EC_{90}$  and  $EC_{99}$   
185 values of 5.4 and 8.4  $\mu\text{M}$ , respectively). Moreover, **10** was 2-  
186 fold more active than ribavirin, a broad antiviral molecule that  
187 was included as a reference molecule. In the vRNP  
188 reconstitution assay, compounds **10**, **11**, and **15** reached  $EC_{50}$   
189 values of 16, 64, and 24  $\mu\text{M}$ , respectively, while the reference  
190 compounds L-742,001 and ribavirin had  $EC_{50}$  values of 3.4 and  
191 8.4  $\mu\text{M}$ , respectively. Hence, compounds **10** and **15** are relevant  
192 candidates for further lead optimization and antiviral/  
193 mechanistic studies.

194 In the last stage, we performed docking using AutoDock 4.2  
195 to predict the PA-Nter binding mode of the three active  
196 molecules, i.e., **10**, **11**, and **15** (Figure 4a). Our results indicate  
197 that their common dihydroxyindole moiety is directed toward  
198 the two catalytic metal ions. The orientation of the metal-  
199 chelating hydroxyl groups appears more favorable for **10** and **11**  
200 compared to **15**. For **10** and **11**, both hydroxyl groups chelate  
201 metal ion B ( $M_B^{2+}$ ) and only one of the hydroxyls interacts with  
202 metal ion A ( $M_A^{2+}$ ). The opposite is seen with **15** because both  
203 its hydroxyl groups are predicted to chelate  $M_A^{2+}$ , while only  
204 one hydroxyl can interact with  $M_B^{2+}$ . Because  $M_B^{2+}$  is generally  
205 considered to be bound with higher affinity compared to  $M_A^{2+}$   
206 (at least when no substrate is present in PA-Nter),<sup>10,22</sup> this  
207 slight difference in orientation may be the basis for the 7-fold  
208 higher potency of **10** compared to **15**. A striking discrepancy  
209 between **11** on the one hand and **10** and **15** on the other hand  
210 involves the compounds' disposition in the cavities surrounding  
211 the active site. **10** and **15** engage opposite pockets compared to  
212 **11**. The catechol functionality of **10** and the second  
213 dihydroxyindole ring of **15** orientate toward the pocket lined  
214 by Val122, Arg124, and Tyr130 (in blue, Figure 4a). In  
215 contrast, **11** binds via its second dihydroxyindole functionality

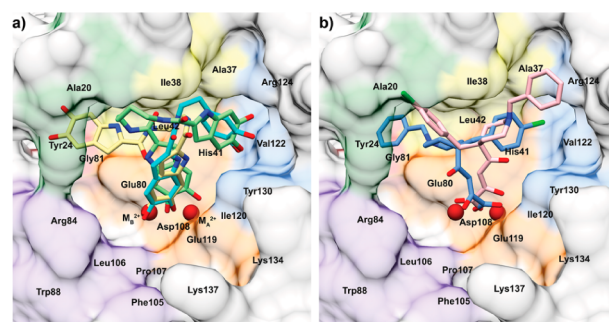


**Figure 4.** Comparison between the predicted poses of **10**, **11**, **15** (a) and L-742,001 (b) obtained by docking into the published<sup>9</sup> structure of inhibitor-free PA-Nter (PDB entry 2W69). The protein structures are shown as surfaces and in the same orientation after structural alignment using the DALI server. The active site metal ions are colored dark red. (a) Superimposition of the best pharmacophore-fitting docking poses obtained for compounds **10** (cyan), **11** (yellow), and **15** (green). (b) Disposition of L-742,001 in PA-Nter as predicted by docking: the conformer representing the most favorable binding energies (in blue) and that representing the most diffuse population of conformers (in pink).<sup>19</sup>

in the pocket surrounded by Ala20, Tyr24, and Gly81 (Figure 216 4a, in green and red). The relevance of the pocket delimited by 217 Val122, Arg124, and Tyr130 was previously proposed in our 218 mutational analysis of the binding pockets of L-742,001 (see 219 Figure 4b).<sup>19</sup> Likewise, this pocket also proved to be of critical 220 importance for the binding of three recently identified PAIs 221 with strong inhibitory activity, as demonstrated in PA-Nter 222 cocrystallization experiments.<sup>18,20</sup> Taken together, our docking 223 results suggest that the superior PA-Nter inhibitory activity of 224 **10** ( $IC_{50} = 0.94 \mu\text{M}$ ) is related to its optimal orientation for 225 metal chelation, combined with its engagement into the 226 Val122–Arg124–Tyr130 cavity. Compound **11** ( $IC_{50}$ : 65 227  $\mu\text{M}$ ) has a similar metal-chelating binding mode yet does not 228 occupy the Val122–Arg124–Tyr130 pocket. The compound 229 with intermediate activity, i.e., **15** ( $IC_{50}$ : 7.0  $\mu\text{M}$ ), is able to 230 occupy the Val122–Arg124–Tyr130 pocket but, compared to 231 **10**, has a less favorable orientation of the metal-chelating 232 functionality. The nice correlation between the results from the 233 enzymatic assay and cell-based (i.e., virus yield and vRNP 234 reconstitution) methods supports our hypothesis that the 235 antiviral activity in cell culture is related to inhibition of PA- 236 Nter. Mechanistic studies are underway to verify this 237 assumption. 238

To summarize, a large database of roughly 5 million 239 structures was screened to identify novel influenza virus 240 endonuclease inhibitors by applying pharmacophore and 241 structure-based docking procedures. Fifteen hits were then 242 evaluated in a PA-Nter enzymatic assay, and three compounds 243 bearing an original bis-dihydroxy-1H-indole-2-carboxamide 244 scaffold demonstrated interesting inhibitory activity, with 245 compounds **10** and **15** having  $IC_{50}$  values in the low 246 micromolar range. Both prototypes also showed antiviral 247 activity in cell-based assays and had comparable potency 248 compared to the reference PAI L-742,001 and the nucleoside 249 analogue inhibitor ribavirin. Follow-up studies are warranted to 250 further assess the full potential of the bis-dihydroxy-1H-indole- 251 2-carboxamide scaffold to develop new influenza PAIs with 252 preclinical relevance. 253

## 254 ■ ASSOCIATED CONTENT

## 255 ● Supporting Information

256 Synthetic and computational procedures. Influenza plasmid-  
257 based endonuclease, virus yield, and vRNP reconstitution  
258 assays. The Supporting Information is available free of charge  
259 on the ACS Publications website at DOI: 10.1021/  
260 acsmedchemlett.5b00109.

## 261 ■ AUTHOR INFORMATION

## 262 Corresponding Authors

263 \*For N.P.: phone, +39 079 228 654; fax, +39 079 229559; E-  
264 mail, nikpal@uniss.it.

265 \*For L.N.: phone, +32-16-337345; E-mail, lieve.naesens@rega.  
266 kuleuven.be.

## 267 Author Contributions

268 The manuscript was written through contributions of all  
269 authors. All authors have given approval to the final version of  
270 the manuscript. N.P. and A.S. contributed equally.

## 271 Funding

272 We thank the Fondazione Banco di Sardegna (grant to M.S.),  
273 the KU Leuven (grant Geconcerteerde Onderzoeksacties,  
274 GOA/15/019/TBA) (to A.S. and L.N.), and the Italian  
275 Ministero dell'Istruzione, dell'Università e della Ricerca  
276 (PRIN 2010, grant 2010W2KM5L\_003) (to M.S, D.R, and  
277 M.C.) for their financial support.

## 278 Notes

279 The authors declare no competing financial interest.

## 280 ■ ACKNOWLEDGMENTS

281 The authors thank Dr. Andrea Brancale for the use of MOE  
282 program. A.S. and L.N. acknowledge Wim van Dam and Ria  
283 Van Berwaer for fine technical assistance, and Meehyein Kim  
284 (Korea Research Institute of Chemical Technology, Daejeon,  
285 South Korea) for generous donation of the vRNP recon-  
286 stitution plasmids.

## 287 ■ ABBREVIATIONS

288 RdRp, RNA-dependent RNA polymerase complex; PA-Nter,  
289 N-terminal part of PA; PAI, PA inhibitor; vRNA, viral RNA;  
290 DKA,  $\beta$ -diketoacid; VS, virtual screening

## 291 ■ REFERENCES

292 (1) *Influenza (Seasonal)—Fact Sheet no. 211*; World Health  
293 Organization: Geneva, 2014; [http://www.who.int/mediacentre/  
294 factsheets/fs211/en/](http://www.who.int/mediacentre/factsheets/fs211/en/) (accessed 19 January 2015).  
295 (2) Uyeki, T. M. Preventing and controlling influenza with available  
296 interventions. *N. Engl. J. Med.* **2014**, *370*, 789–791.  
297 (3) Vanderlinden, E.; Naesens, L. Emerging antiviral strategies to  
298 interfere with influenza virus entry. *Med. Res. Rev.* **2014**, *34*, 301–339.  
299 (4) Leang, S. K.; Deng, Y. M.; Shaw, R.; Caldwell, N.; Iannello, P.;  
300 Komadina, N.; Buchy, P.; Chittaganpitch, M.; Dwyer, D. E.; Fagan, P.;  
301 Gourinat, A. C.; Hammill, F.; Horwood, P. F.; Huang, Q. S.; Ip, P. K.;  
302 Jennings, L.; Kesson, A.; Kok, T.; Kool, J. L.; Levy, A.; Lin, C.; Lindsay,  
303 K.; Osman, O.; Papadakis, G.; Rahnamal, F.; Rawlinson, W.; Redden,  
304 C.; Ridgway, J.; Sam, I. C.; Svobodova, S.; Tandoc, A.;  
305 Wickramasinghe, G.; Williamson, J.; Wilson, N.; Yusof, M. A.; Kelso,  
306 A.; Barr, I. G.; Hurt, A. C. Influenza antiviral resistance in the Asia-  
307 Pacific region during 2011. *Antiviral Res.* **2013**, *97*, 206–210.  
308 (5) Ruigrok, R. W.; Crépin, T.; Hart, D. J.; Cusack, S. Towards an  
309 atomic resolution understanding of the influenza virus replication  
310 machinery. *Curr. Opin. Struct. Biol.* **2010**, *20*, 104–113.

(6) Pflug, A.; Guilligay, D.; Reich, S.; Cusack, S. Structure of 311  
influenza A polymerase bound to the viral RNA promoter. *Nature* 312  
**2014**, *516*, 355–360. 313

(7) Reich, S.; Guilligay, D.; Pflug, A.; Malet, H.; Berger, I.; Crépin, 314  
T.; Hart, D.; Lunardi, T.; Nanao, M.; Ruigrok, R. W.; Cusack, S. 315  
Structural insight into cap-snatching and RNA synthesis by influenza 316  
polymerase. *Nature* **2014**, *516*, 361–366. 317

(8) Plotch, S. J.; Bouloy, M.; Ulmanen, I.; Krug, R. M. A unique 318  
cap(m<sup>7</sup>GpppXm)-dependent influenza virion endonuclease cleaves 319  
capped RNAs to generate the primers that initiate viral RNA 320  
transcription. *Cell* **1981**, *23*, 847–858. 321

(9) Dias, A.; Bouvier, D.; Crépin, T.; McCarthy, A. A.; Hart, D. J.; 322  
Baudin, F.; Cusack, S.; Ruigrok, R. W. The cap-snatching endonuclease 323  
of influenza virus polymerase resides in the PA subunit. *Nature* **2009**, 324  
*458*, 914–918. 325

(10) Yuan, P.; Bartlam, M.; Lou, Z.; Chen, S.; Zhou, J.; He, X.; Lv, Z.; 326  
Ge, R.; Li, X.; Deng, T.; Fodor, E.; Rao, Z.; Liu, Y. Crystal structure of 327  
an avian influenza polymerase PA(N) reveals an endonuclease active 328  
site. *Nature* **2009**, *458*, 909–913. 329

(11) Das, K.; Aramini, J. M.; Ma, L. C.; Krug, R. M.; Arnold, E. 330  
Structures of influenza A proteins and insights into antiviral drug 331  
targets. *Nature Struct. Mol. Biol.* **2010**, *17*, 530–538. 332

(12) Rogolino, D.; Carcelli, M.; Sechi, M.; Neamati, N. Viral enzymes 333  
containing magnesium: metal binding as a successful strategy in drug 334  
design. *Coord. Chem. Rev.* **2012**, *256*, 3063–3086. 335

(13) Tomassini, J. E.; Selnick, H.; Davies, M. E.; Armstrong, M. E.; 336  
Baldwin, J.; Bourgeois, M.; Hastings, J. C.; Hazuda, D.; Lewis, J.; 337  
McClements, W.; Ponticello, G.; Radzilowski, E.; Smith, G.; Tebben, 338  
A.; Wolfe, A. Inhibition of cap (m<sup>7</sup>GpppXm)-dependent endonuclease 339  
of influenza virus by 4-substituted 2,4-dioxobutanoic acid compounds. 340  
*Antimicrob. Agents Chemother.* **1994**, *38*, 2827–2837. 341

(14) Hastings, J. C.; Selnick, H.; Wolanski, B.; Tomassini, J. E. Anti- 342  
influenza virus activities of 4-substituted 2,4-dioxobutanoic acid 343  
inhibitors. *Antimicrob. Agents Chemother.* **1996**, *40*, 1304–1307. 344

(15) Tomassini, J. E.; Davies, M. E.; Hastings, J. C.; Lingham, R.; 345  
Mojena, M.; Raghooobar, S. L.; Singh, S. B.; Tkacz, J. S.; Goetz, M. A. A 346  
novel antiviral agent which inhibits the endonuclease of influenza 347  
viruses. *Antimicrob. Agents Chemother.* **1996**, *40*, 1189–1193. 348

(16) Cianci, C.; Chung, T. D. Y.; Meanwell, N.; Putz, H.; Hagen, M.; 349  
Colonna, R. J.; Krystal, M. Identification of N-hydroxamic acid and N- 350  
hydroxy-imide compounds that inhibit the influenza virus polymerase. 351  
*Antiviral Chem. Chemother.* **1996**, *7*, 353–360. 352

(17) Singh, S. B.; Tomassini, J. E. Synthesis of natural flutimide and 353  
analogous fully substituted pyrazine-2,6-diones, endonuclease inhib- 354  
itors of influenza virus. *J. Org. Chem.* **2001**, *66*, 5504–5516. 355

(18) Bauman, J. D.; Patel, D.; Baker, S. F.; Vijayan, R. S.; Xiang, A.; 356  
Parhi, A. K.; Martínez-Sobrido, L.; Lavoie, E. J.; Das, K.; Arnold, E. 357  
Crystallographic fragment screening and structure-based optimization 358  
yields a new class of influenza endonuclease inhibitors. *ACS Chem.* 359  
*Biol.* **2013**, *8*, 2501–2508. 360

(19) Stevaert, A.; Dallochio, R.; Dessi, A.; Pala, N.; Rogolino, D.; 361  
Sechi, M.; Naesens, L. Mutational analysis of the binding pockets of 362  
the diketo acid inhibitor L-742,001 in the influenza virus PA 363  
endonuclease. *J. Virol.* **2013**, *87*, 10524–10538. 364

(20) Sagong, H. Y.; Bauman, J. D.; Patel, D.; Das, K.; Arnold, E.; 365  
Lavoie, E. J. Phenyl substituted 4-hydroxypyridazin-3(2H)-ones and 5- 366  
hydroxypyrimidin-4(3H)-ones: inhibitors of influenza A endonuclease. 367  
*J. Med. Chem.* **2014**, *57*, 8086–8098. 368

(21) Kuzuhara, T.; Iwai, Y.; Takahashi, H.; Hatakeyama, D.; Echigo, 369  
N. Green tea catechins inhibit the endonuclease activity of influenza A 370  
virus RNA polymerase. *PLoS Curr.* **2009**, *1*, RRN1052. 371

(22) Xiao, S.; Klein, M. L.; LeBard, D. N.; Levine, B. G.; Liang, H.; 372  
MacDermaid, C. M.; Alfonso-Prieto, M. Magnesium-dependent RNA 373  
binding to the PA endonuclease domain of the avian influenza 374  
polymerase. *J. Phys. Chem. B* **2014**, *118*, 873–889. 375

(23) Berman, H. M.; Westbrook, J.; Feng, Z.; Gilliland, G.; Bhat, T. 376  
N.; Weissig, H.; Shindyalov, I. N.; Bourne, P. E. The Protein Data 377  
Bank. *Nucleic Acids Res.* **2000**, *28*, 235–242. 378

- 379 (24) Baughman, B. M.; Jake Slavish, P.; DuBois, R. M.; Boyd, V. A.;  
380 White, S. W.; Webb, T. R. Identification of influenza endonuclease  
381 inhibitors using a novel fluorescence polarization assay. *ACS Chem.*  
382 *Biol.* **2012**, *7*, 526–534.
- 383 (25) Carcelli, M.; Rogolino, D.; Bacchi, A.; Rispoli, G.; Fiscaro, E.;  
384 Compari, C.; Sechi, M.; Stevaert, A.; Naesens, L. Metal-chelating 2-  
385 hydroxyphenyl amide pharmacophore for inhibition of influenza virus  
386 endonuclease. *Mol. Pharmaceutics* **2014**, *11*, 304–316.
- 387 (26) Stevaert, A.; Nurra, S.; Pala, N.; Carcelli, M.; Rogolino, D.;  
388 Shepard, C.; Domaol, R. A.; Kim, B.; Alfonso-Prieto, M.; Marras, S. A.  
389 E.; Sechi, M.; Naesens, L. An integrated biological approach to guide  
390 the development of metal-chelating inhibitors of influenza virus PA  
391 endonuclease. *Mol. Pharmacol.* **2015**, *87*, 323–337.
- 392 (27) Walters, W. P.; Stahl, M. T.; Murcko, M. A. Virtual screening—  
393 an overview. *Drug Discovery Today* **1998**, *3*, 160–178.
- 394 (28) Jorgensen, W. L. The many roles of computation in drug  
395 discovery. *Science.* **2004**, *303*, 1813–1818.
- 396 (29) Pala, N.; Dallochio, R.; Dessi, A.; Brancale, A.; Carta, F.; Ihm,  
397 S.; Maresca, A.; Sechi, M.; Supuran, C. T. Virtual screening-driven  
398 identification of human carbonic anhydrase inhibitors incorporating an  
399 original, new pharmacophore. *Bioorg. Med. Chem. Lett.* **2011**, *21*,  
400 2515–2520.
- 401 (30) Ishikawa, Y.; Fujii, S. Binding mode prediction and inhibitor  
402 design of anti-influenza virus diketo acids targeting metalloenzyme  
403 RNA polymerase by molecular docking. *Bioinformatics* **2011**, *6*, 221–  
404 225.
- 405 (31) Yan, Z.; Zhang, L.; Fu, H.; Wang, Z.; Lin, J. Design of the  
406 influenza virus inhibitors targeting the PA endonuclease using 3D-  
407 QSAR modeling, side-chain hopping, and docking. *Bioorg. Med. Chem.*  
408 *Lett.* **2014**, *24*, 539–547.
- 409 (32) Parkes, K. E.; Ermert, P.; Fässler, J.; Ives, J.; Martin, J. A.;  
410 Merrett, J. H.; Obrecht, D.; Williams, G.; Klumpp, K. Use of a  
411 pharmacophore model to discover a new class of influenza  
412 endonuclease inhibitors. *J. Med. Chem.* **2003**, *46*, 1153–1164.
- 413 (33) Kim, J.; Lee, C.; Chong, Y. Identification of potential influenza  
414 virus endonuclease inhibitors through virtual screening based on the  
415 3D-QSAR model. *SAR QSAR Environ. Res.* **2009**, *20*, 103–118.
- 416 (34) *Molecular Operating Environment, MOE 2009.10*; Chemical  
417 Computing Group Inc.: 1010 Sherbooke St. West, Suite #910,  
418 Montreal, QC, Canada, H3A 2R7, 2009.
- 419 (35) Sechi, M.; Angotzi, G.; Dallochio, R.; Dessi, A.; Carta, F.;  
420 Sannia, L.; Mariani, A.; Fiori, S.; Sanchez, T.; Movsessian, L.; Plasencia,  
421 C.; Neamati, N. Design and synthesis of novel dihydroxyindole-2-  
422 carboxylic acids as HIV-1 integrase inhibitors. *Antiviral Chem.*  
423 *Chemother.* **2004**, *15*, 67–81.
- 424 (36) Sechi, M.; Azzena, U.; Delussu, M. P.; Dallochio, R.; Dessi, A.;  
425 Cosseddu, A.; Pala, N.; Neamati, N. Design and synthesis of bis-amide  
426 and hydrazide-containing derivatives of malonic acid as potential HIV-  
427 1 integrase inhibitors. *Molecules* **2008**, *13*, 2442–2461.
- 428 (37) Sechi, M.; Rizzi, G.; Bacchi, A.; Carcelli, M.; Rogolino, D.; Pala,  
429 N.; Sanchez, T.; Taheri, L.; Dayam, R.; Neamati, N. Design and  
430 synthesis of novel dihydroxyquinoline-3-carboxylic acids as HIV-1  
431 integrase inhibitors. *Bioorg. Med. Chem. Lett.* **2009**, *17*, 2925–2935.